

# In vitro and in vivo evaluation of an intraocular implant for glaucoma treatment

Mădălina V. Natu<sup>a</sup>, Manuel N. Gaspar<sup>b</sup>, Carlos A. Fontes Ribeiro<sup>b</sup>,  
António M. Cabrita<sup>c</sup>, Hermínio C. de Sousa<sup>a</sup>, M. H. Gil<sup>a,1,\*</sup>

<sup>a</sup>*Department of Chemical Engineering, University of Coimbra, Pólo II, 3030-790, Coimbra, Portugal*

<sup>b</sup>*Institute of Pharmacology and Experimental Therapeutics, University of Coimbra, Pólo III, 3000-354, Coimbra, Portugal*

<sup>c</sup>*Institute of Experimental Pathology, University of Coimbra, Pólo I, 3004-504, Coimbra, Portugal*

---

## Abstract

Implantable disks for glaucoma treatment were prepared by blending poly( $\epsilon$ -caprolactone), PCL, poly(ethylene oxide)-*b*-poly(propylene oxide)-*b*-poly(ethylene oxide) and dorzolamide. Their in vivo performance was assessed by their capacity to decrease intraocular pressure (IOP) in normotensive and hypertensive eyes. Drug mapping showed that release was complete from blend disks and the low molecular weight (MW) PCL after 1 month in vivo. The high MW PCL showed non-cumulative release rates above the therapeutic level during 3 months in vitro. In vivo, the fibrous capsule formation around the implant controls the drug release, working as a barrier membrane. Histologic analysis showed normal foreign body reaction response to the implants. In normotensive eyes, a 20 % decrease in IOP obtained with the disks during 1 month was similar to Trusopt<sup>®</sup> eyedrops treatment. In hypertensive eyes, the most sustained decrease was shown by the high MW PCL (40 % after 1 month, 30 % after 2 months). It was shown that the implants can lower IOP in sustained manner in a rabbit glaucoma model.

*Keywords:* poly( $\epsilon$ -caprolactone), subconjunctival implant, controlled drug release, in vivo, intraocular pressure, glaucoma

---

\*Corresponding author

*Email address:* hgil@eq.uc.pt (M. H. Gil)

<sup>1</sup>tel:+351239798700, fax:+351239798703

---

## 1. Introduction

Glaucoma is a chronic condition that requires long-term treatment in order to stop progressive and irreversible blindness ([1]). Treatment of glaucoma focuses on preserving vision by slowing down damage to the optic nerve. Therapy aims at preventing further damage by lowering IOP (or ocular hypertension) and it usually consists of pharmaceutical treatment and laser or surgical procedures ([2]). It was shown that reducing IOP is effective in preventing disease progression in ocular hypertension, primary open angle glaucoma, and even in normal tension glaucoma ([3]).

In most glaucoma patients, medical therapy consists of topical eyedrops and oral tablets. However, administration and compliance are often problematic. Eyedrops produce low ocular bioavailability ([4]), unnecessary systemic exposure ([5]) and have low patient compliance due to uncomfortable sensations ([6]), as well as difficulty of instillation or forgetfulness ([7]). Two main strategies have already been used clinically to diminish such effects, namely gel forming (viscous) solutions ([8]) and controlled drug delivery systems (CDDS).

CDDS in the form of intraocular implants can deliver therapeutically effective amounts of drugs to targeted ocular tissues over sustained period of time without significant ocular/systemic side effects ([9]). Thus, CDDS can extremely suitable for chronic diseases, which require a constant level of medication to be maintained in the body over a long period of time. The major motivation for development and use of these devices is that they eliminate the need to take multiple doses of a drug during the day or week, thereby improving patient compliance and therapy outcomes ([4]).

In a previous work, implants based on poly( $\epsilon$ -caprolactone), PCL were prepared by solvent-casting, followed by dip-coating ([10]). Unfortunately, this preparation method is not reproducible and low drug loadings were achieved. High drug loads are needed for long term treatment of chronic diseases such as glaucoma. Moreover, the volume of such devices should be as small as possible in order to be easily introduced at the implantation site. Melt compression is a reproducible, easily scalable method of producing implants of different shapes and sizes ([11, 12]). In addition, compact implants can be obtained with small polymer-to-drug ratio, which enables high drug loads in a relatively small implant volume.

36 The objective of the present work was to prepare a drug loaded biodegrad-  
37 able implant designed to provide a localized, long-term (6 months to 2 years)  
38 sustained release of the drug, that can be used in the treatment of glaucoma.  
39 A subconjunctival placement of the implant is simple to perform because of  
40 easy access to the implantation area and low vascularization. PCL and Lutrol  
41 F 127, Lu were selected because they are both biocompatible, biodegradable  
42 and they can be easily processed by conventional polymer processing tech-  
43 niques ([13]). Moreover, they are commercially available, inexpensive and  
44 well characterised polymers. PCL is a slowly degradable polymer, while Lu  
45 can be used as a release modulator ([14, 15]). Two molecular weights of PCL  
46 were used because it was shown that molecular weight determines the time  
47 lag before erosion and the rate of bioerosion in vivo ([16]). The implantable  
48 drug loaded disks were prepared by melt compression and their performance  
49 in vivo was evaluated by assessing the capacity to lower IOP in normotensive  
50 and hypertensive rabbit eyes.

## 51 **2. Materials and methods**

### 52 *2.1. Preparation of polymer disks*

53 Poly( $\epsilon$ -caprolactone) (PCL40, average  $M_w$  65000 g/mol and PCL10, aver-  
54 erage  $M_w$  15000 g/mol, Sigma-Aldrich) and Lutrol F 127 (Lu, poly(ethylene  
55 oxide)-b-poly(propylene oxide)-b-poly(ethylene oxide), 9000-14000 g/mol, 70  
56 % by weight of polyoxyethylene, BASF) films and dorzolamide hydrochloride  
57 (Chemos GmbH) loaded films (Lu/PCL: 13/87, 6/94, 0/100 % w/w) were  
58 prepared by solvent casting from acetone (UV grade, Sigma-Aldrich) at 40  
59 °C, using a 15 % w/v total polymer concentration and 33.3 % w/w theoret-  
60 ical drug loading. Polymer sheets were fabricated by compression moulding  
61 of the polymer films in a stainless steel mould by applying a pressure of 201.5  
62 kg/m<sup>2</sup> for 20 minutes at 100°C. The mould was subsequently cooled under  
63 a jet of cold water (20°C) during 2 minutes. Discs of 4 mm diameter (1 mm  
64 thickness, 4-5 mg drug mass, 13-16 mg total mass) were punched from the  
65 polymer sheets. They were used as such in characterization tests. Prior to  
66 in vivo implantation, the discs were sterilized using UV radiation during 20  
67 minutes (at 254 nm) in a UV chamber (Camag UV cabinet).

### 68 *2.2. Disk characterization*

69 Differential scanning calorimetry (DSC) was carried out using a DSC  
70 Q100 equipment (TA Instruments) under nitrogen atmosphere (100 mL/min).

71 Samples with masses of approximately 5 mg were heated until 100°C, at a  
72 heating rate of 10°C/min. The relative crystallinity of the disks was cal-  
73 culated as previously described considering the melting enthalpy of 100 %  
74 crystalline PCL and 100 % crystalline Lu [15]. Thermogravimetric analysis  
75 (TGA) was carried out using a SDT Q 600 equipment (TA Instruments).  
76 Samples with masses of approximately 10 mg were heated until 600°C, at a  
77 heating rate of 10°C/min. The degradation temperature ( $T_d$ ) was determined  
78 at the onset point of the TGA plot.

79 Water contact angle was evaluated by static contact angle measurements  
80 using an OCA 20 Video-Based Contact Angle Meter (Dataphysics) and em-  
81 ploying the sessile drop method.

82 Drug loading of the disks was assessed by elemental analysis (quantifica-  
83 tion of sulphur, present only in the drug molecule).

### 84 *2.3. Morphology and drug distribution*

85 The morphology of the disks (before and after implantation) was exam-  
86 ined using scanning electron microscopy, SEM (JSM 5310, Jeol). The drug  
87 mapping (elemental sulphur) of the disks surface and cross-section (showing  
88 the center of the disk) was done using electron probe microanalysis, EPMA  
89 (Camebax SX50, Cameca) at 15 kV accelerated voltage and 40 nA probe  
90 current.

### 91 *2.4. In vitro and in vivo degradation*

92 The extent of hydrolytic degradation of the disks (as prepared, in vitro  
93 degraded and in vivo degraded) was evaluated by determining the change  
94 of MW in time. Polymer disks were placed in 4 mL PBS with 0.001 %  
95 sodium azide, at 37°C. The changes in the MW were measured by size ex-  
96 clusion chromatography (SEC), using chloroform as mobile phase (1 ml/min,  
97 30 °C) and a PLgel MIXED-C column (300 mm×7.5 mm, 5 μm, Varian).  
98 PL-EMD 960 (Polymer Laboratories) evaporative light scattering detector  
99 was used to acquire the data. Universal calibration was performed us-  
100 ing polystyrene (PS) standards and Mark-Houwink parameters  $k_{PCL}=1.09$   
101  $\times 10^{-3}$  dl/g,  $\alpha_{PCL}=0.60$ ,  $k_{PS}=1.25 \times 10^{-4}$  dl/g,  $\alpha_{PS}=0.71$ . Peak integration  
102 was performed using Clarity chromatography software (DataApex).

### 103 *2.5. In vitro drug release and release modelling*

104 Dorzolamide hydrochloride release was studied in 10 ml phosphate saline  
105 buffer medium (PBS tablets, pH 7.4, 10 mM phosphate, 137 mM sodium,

106 2.7 mM potassium, Sigma-Aldrich) at 37°C. At scheduled time intervals,  
 107 samples were taken and the entire medium volume was replaced with fresh  
 108 medium to maintain sink conditions. The mass of dorzolamide hydrochloride  
 109 released at time  $t$  was determined by UV spectroscopy at 254 nm (Jasco  
 110 V-650 Spectrophotometer). The percentage of in vitro released drug was  
 111 calculated using Eq.1.

$$\text{Released drug in vitro (\%)} = \frac{M_{dt}}{M_{d0}} \times 100 \quad (1)$$

112 In Eq. 1,  $M_{dt}$  is the drug mass released at time  $t$  and  $M_{d0}$  is the initial drug  
 113 mass.

114 In order to study the drug release mechanism, the power law equation  
 115 (Eq.2) which is based on diffusional model of drug transport, was used, where  
 116  $M_t/M_{total}$  is the fractional release of the drug,  $k$  is the kinetic constant and  
 117  $n$  is the release exponent, indicating the mechanism of drug release [15].

$$\frac{M_t}{M_{total}} = k t^n \quad (2)$$

118 An alternative model (Eq.3) based on polymer degradation control of  
 119 drug release was used to fit the release data. In this model, two pools of  
 120 drug are considered: a pool of mobile drug which readily diffuses out of the  
 121 matrix upon immersion in an aqueous medium and a pool of immobilized  
 122 drug which can diffuse only after matrix degradation [15]. This model can  
 123 be applied to slow-degrading polymers such as PCL due to the fact that  
 124 polymer degradation is much slower than drug diffusion and as such it is the  
 125 rate limiting step for drug transport.

$$M(\tau) = A_0 + |\Omega| S_0 (1 - \exp(-\tau)), \bar{\alpha}_{lmn}^{-1} \rightarrow 0 \quad (3)$$

126 In Eq. 3,  $A_0$  is the load of the mobile drug,  $S_0$  is the load of immobilized  
 127 drug,  $\tau$  is the dimensionless time and is defined by  $\tau = \mu t$  ( $\mu$  is the degrada-  
 128 tion rate constant) and  $\Omega$  is the geometrical factor. The model parameters  
 129 were determined by non-linear regression and the goodness of the fit was  
 130 assessed.

### 131 2.6. Disk implantation, glaucoma model, intraocular pressure measurement 132 and in vivo drug release

133 New Zealand white rabbits were used in animal experiments in agree-  
 134 ment with European Union Council Directive 86/609/EEC regarding the

135 protection of animals used for experimental and other scientific purposes as  
136 described before ([10]). The disk implantation procedure and the IOP mea-  
137 surement by tonometry were already described ([10]). In order to produce  
138 high IOP, we used a low temperature ophthalmic cautery (Bovie, Aaron Med-  
139 ical) to produce 30 to 50 burns that were directed at the limbal plexus and  
140 at the episcleral veins ([17, 18]).

141 The animals were divided in three groups: group 1 (n=26) received drug  
142 loaded polymer disks (the right eye contained the drug loaded disk-PCL40,  
143 PCL10, 6%Lu,PCL40 and 13%Lu,PCL40, while the left had the control disk-  
144 polymers without drug), group 2 (n=3) was submitted to Trusopt<sup>®</sup> eyedrops  
145 (dorzolamide hydrochloride 2 %, Chibret) treatment (1 drop twice a day in  
146 the right eye, while the left eye received a drop of balanced salt solution,  
147 BSS sterile solution, Alcon), while group 3 (n=3) was the glaucoma model  
148 reference.

149 For in vivo release tests, previously weighed polymer disks were implanted  
150 as described before for predetermined periods of time and subsequently re-  
151 moved, cleaned of ocular tissues, rinsed with distilled water and vacuum-dried  
152 to constant weight. The in vivo released mass of drug was determined gravi-  
153 metrically using Eq. 4. In Eq. 4,  $M_i$  is the initial disk mass,  $M_t$  is the disk  
154 mass after implantation time  $t$ ,  $M_c$  is the mass loss of the control disk and  
155  $M_{d0}$  is the initial drug mass.

$$\text{Released drug in vivo (\%)} = \frac{M_i - M_t - M_c}{M_{d0}} \times 100 \quad (4)$$

156 In vivo drug released percentages were also determined by elemental anal-  
157 ysis (the residual drug was determined after in vivo implantation).

### 158 2.7. Histologic evaluation

159 The local implant site and important organs were excised for histological  
160 evaluation. The collected organs included kidneys, spleen, liver, lung (only  
161 after 2 months implantation). The organs and tissue samples were fixed in  
162 10 % neutral buffered formaldehyde. The samples were then embedded in  
163 paraffin and dehydrated by isopropanol processing. Thin layers were cut  
164 from the samples with a microtome and stained with hematoxylin and eosin  
165 for optical microscopy.

Sample	$T_d$ ( $^{\circ}C$ )	$T_m$ ( $^{\circ}C$ )	Contact angle (deg)
PCL40+drug	279.38, 420.20	61.53 (0.03)	80.23 (2.63)
PCL40	375.51	61.26 (0.31)	73.88 (3.31)
PCL10+drug	275.00, 420.33	60.67 (0.19)	78.26 (1.24)
PCL10	269.62, 421.88	61.23 (0.61)	70.24 (1.86)
6%Lu,PCL40+drug	-	61.45 (0.42)	46.87 (2.78)
6%Lu,PCL40	-	62.07 (0.17)	32.52 (2.12)
13%Lu,PCL40+drug	-	58.22 (0.26)	39.88 (0.80)
13%Lu,PCL40	-	58.86 (0.45)	40.20 (2.53)
Lu	358.80	55.57 (0.65)	59.33 (0.35)

Table 1: Water contact angle, melting and degradation temperatures of the disks

166 *2.8. Statistics*

167 All values are presented as mean and standard error of the mean (SEM).  
168 Experiments were performed in triplicates. Statistical analysis (Student's  
169 T-test, independent, two-tailed) was done using OpenOffice.org Calc 3.1.

170 **3. Results and discussion**

171 *3.1. Disk characterization*

172 In Table 1, melting ( $T_m$ ) and degradation temperatures ( $T_d$ ) are presented  
173 for drug loaded and control disks because their knowledge is required when  
174 dealing with polymer processing methods for the manufacture of drug-eluting  
175 implants. Blend disks are more hydrophilic than PCL disks due to the in-  
176 corporation of hydrophilic Lu ([14, 15]) as shown by the lower contact angle  
177 values. The low  $T_m$  enables processing at temperatures much lower than the  
178 degradation temperature of dorzolamide ( $T_d=251.26^{\circ}C$ ). The PCL samples  
179 show a two step degradation process, the first step corresponding to drug  
180 degradation, while the second corresponds to polymer degradation.

181 All disks presented an average content of sulphur of 33.6 %, which corre-  
182 sponds to approximately 5 mg of loaded drug in each disk.

183 *3.2. General considerations about implantation surgical procedure and animal  
184 wellbeing*

185 The surgical procedure to insert the disks is relatively easy to perform  
186 because of easy access to the implantation area and low vascularization.

187 Moreover, the wound does not need to be sutured because a pocket is cre-  
188 ated that keeps the disk in place. The fixation of the disk is further enhanced  
189 by fast wound healing as the disk is completely encapsulated by the conjunctiva.  
190 Ocular adverse events included conjunctivitis (6 eyes in 64 eyes), that  
191 resolved clinically in less than 1 week (with antibiotic eyedrops). No other  
192 events were observed. It should be mentioned that such ocular adverse events  
193 (conjunctival hyperemia, stinging, burning, foreign body sensation, tearing,  
194 vision blurring) are quite frequent in topical treatment with eyedrops [6].

### 195 3.3. *In vitro and in vivo drug release*

196 Each disk was loaded with approximately 5 mg of drug in order to achieve  
197 a release rate of 18  $\mu\text{g}/\text{day}$  (similar with the one obtained with Trusopt<sup>®</sup>  
198 2% instillation three times a day [19]) for at least 4.5 months (we considered  
199 50 % drug losses during the transport from conjunctiva to ciliary body).

200 Fig. 1(a) presents the release from blends: release is almost complete  
201 after 10 days for 13%Lu,PCL40 and after 20 days for 6%Lu,PCL40. The  
202 release kinetics shown in Fig. 1(b) presents similar released drug percentages  
203 regardless of the PCL molecular weight.

204 A comparison between released drug percentages in vitro and in vivo  
205 is shown in Table 2. It can be noted that there are significant differences  
206 between released percentages in vitro and in vivo for PCL40 and PCL10  
207 samples ( $p=0.07$  and  $p=0.01$ , respectively), while the released drug percent-  
208 ages of 6%Lu,PCL40 and 13%Lu,PCL40 are similar in vitro and in vivo  
209 ( $p=0.15$  for 6%Lu,PCL40). In vivo drug released percentages (calculated by  
210 mass balance) for PCL40 implant were confirmed by elemental analysis (the  
211 residual drug was determined after in vivo implantation): after 8 days, 22.69  
212 (5.82) % released drug, after 14 days, 24.09 (2.93) % released drug and after  
213 22 days 35.74 (11.54) % released drug.

214 In vivo release kinetics (Fig. 1(c)) seems to approach a zero-order kinetics,  
215 while the in vitro kinetics curves (Fig. 1(b)) appear to have a  $t^{0.5}$  profile.  
216 This may be due to different release controlling phenomena: in vitro, diffusion  
217 controls drug release (from here the classic, Fickian  $t^{0.5}$  profile), while in vivo,  
218 the fibrous capsule formation around the implant (see section 3.7) controls  
219 the drug release, functioning as a barrier membrane that slows down release.  
220 Thus, there should be significant differences between drug released in vitro  
221 and in vivo (see Table 2) for PCL40 and PCL10 samples. For blend samples,  
222 due to polymer erosion that takes place mostly in the first day of release  
223 [15], the fibrous capsule/barrier control is absent (only after 1 week, the



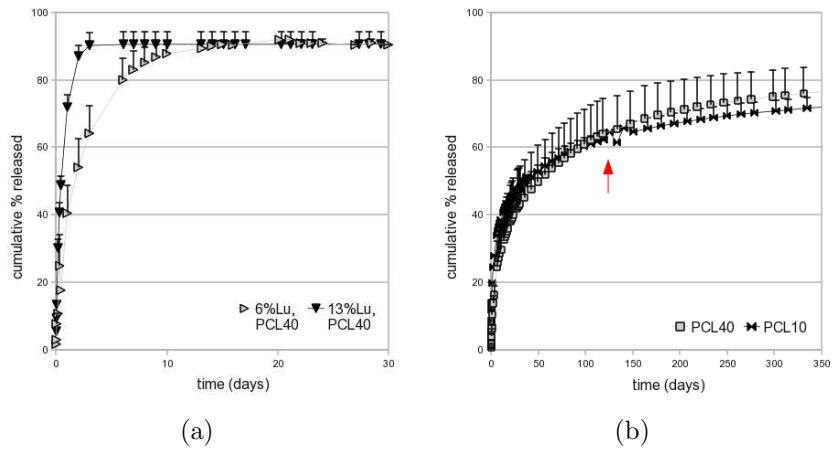


Figure 1: a), b) In vitro drug release (the red arrow indicates the point on the kinetics curve when the released dose is smaller than the effective dose), c) Comparison between in vivo and in vitro drug release for sample PCL40

Sample	In vitro		In vivo			
	Rel. drug (%)		Rel. drug mass (mg)		Rel. drug (%)	
	1 month	2 months	1 month	2 months	1 month	2 months
PCL40	40.14 (6.48)	51.88 (6.07)*	2.22 (0.72)	3.72 (0.13)	42.99 (14.06)	72.02 (2.49)*
PCL10	47.29 (0.96)*	-	4.47 (0.18)	-	83.30 (4.01)*	-
6%Lu,PCL40	90.98 (1.06)	-	4.74 (0.20)	-	96.80 (1.62)	-
13%Lu,PCL40	90.57 (3.79)	-	4.95	-	94.56	-

Table 2: Released drug percentages for in vitro tested disks and disks implanted during 1 month or 2 months (\*,  $p \leq 0.1$  statistically significant differences between in vitro and in vivo drug released percentages)

224 disks were fully encapsulated) and as such the released drug percentages are  
225 similar both in vitro and in vivo.

226 In Table 3, the non-linear regression results are presented. The objec-  
227 tive behind fitting these equations to the release data was to understand  
228 the underlying phenomena involved in the drug release mechanism. Smaller  
229 values for  $S_0$  suggest higher amounts of immobilized drug that will not be  
230 released (37.8 % for PCL40 and 16.6 % for 13%Lu,PCL40). The percentage  
231 of immobilized drug is higher for PCL40 than for blend samples because in  
232 the latter case erosion creates more surface area and exposes more drug to  
233 water dissolution that otherwise would be trapped. In the case of the studied  
234 polymers, physical immobilization of the drug occurs due to drug entrapment  
235 in crystalline regions. Drug diffusion from these regions is hindered because  
236 water enters initially only in the amorphous parts. The immobilized fraction  
237 of the drug will be released only with polymer degradation (this explains  
238 why the steady state value of released drug percentage is smaller than 100  
239 %, which would correspond to total release).

240 The regression results obtained using power law equation reinforce the  
241 previous observations. The high value of  $k$  indicates the extent of burst,  
242 higher for blend samples. The range of values for the release exponent is

Sample	Power law			Degradation model			
	$k$ (day <sup>-n</sup> )	$n$	$R_{adj}^2$	$A_0$	$S_0$	$\mu$ (day <sup>-1</sup> )	$R_{adj}^2$
PCL40	17.05 (0.65)	0.26 (0.01)	0.98	10.75 (1.42)	62.21 (1.64)	0.02 (0.00)	0.96
PCL10	24.11 (0.60)	0.19 (0.01)	0.97	15.86 (1.67)	51.45 (1.86)	0.04 (0.00)	0.92
6%Lu,PCL40	41.31 (3.14)	0.27 (0.03)	0.92	5.90 (1.33)	84.12 (1.46)	0.42 (0.03)	0.99
13%Lu,PCL40	56.23 (3.53)	0.17 (0.02)	0.83	7.01 (0.66)	83.41 (0.69)	1.66 (0.04)	1.00

Table 3: Model parameters determined by non-linear regression

243 indicative of a diffusion mechanism for drug release. This model fails to  
244 explain the last stage of the release (steady-state at less than 100 % released  
245 drug) as it doesn't consider the effect of polymer degradation.

246 The release kinetics suggested a three stage release mechanism, with  
247 different steps depending on disk composition. Dissolution of the surface  
248 loaded drug and subsequent diffusion, followed by diffusion of the mobile  
249 drug through water-filled pores (created either due to Lu leaching or poly-  
250 mer recrystallization [15, 20]), while the last stage was controlled by polymer  
251 degradation and subsequent diffusion of the immobilized drug. In blends,  
252 most of the drug is released due to polymer erosion, while the residual drug  
253 was released by diffusion through water-filled pores. The mechanism from  
254 PCL40/PCL10 disks and blend disks are essentially the same, except for the  
255 initial stage when drug diffusion is coupled with polymer erosion in the case  
256 of blends. By selecting the proper ratio between the components, the pre-  
257 ponderance of a certain stage during drug release can be changed, obtaining  
258 an overall effect in drug release that fits the intended application.

### 259 3.4. Intraocular pressure measurement

260 In order to simulate ocular hypertension, we developed a rabbit glaucoma  
261 model by increasing the IOP values (Fig. 2(d)) from an average of 20.9 mmHg  
262 (normotensive eyes) to an average of 30.1 mmHg (hypertensive eyes). A  
263 second procedure was performed after 1 month because IOP values returned

Sample	Average IOP reduction (%)		
	Normotensive eyes	Hypertensive eyes	
	1 month	1 month	2 months
Trusopt	16.55 (10.94)	25.21 (9.74)	23.82 (10.14)
PCL40	16.91 (6.43)	41.06 (12.16)*	33.21 (8.90)
PCL10	23.73 (8.15)	39.61 (11.90)*	-
6%Lu,PCL40	23.85 (7.24)	39.24 (15.21)*	-
13%Lu,PCL40	16.59 (8.02)	-	-

Table 4: Average IOP reduction (\*,  $p \leq 0.01$  statistically significant differences between IOP percentages obtained by disk implantation relative to those obtained with Trusopt instillation)

264 to baseline after this period [17, 18]. Disks were first tested in normotensive  
265 eyes in order to select the best performing systems. In Fig. 2(e) and Fig. 2(f),  
266 it can be seen that sample 13%Lu,PCL40 decreased IOP by 16.6 % (see also  
267 Table 4) reaching the baseline value after 15 days, while sample 6%Lu,PCL40  
268 decreased IOP by 23.8 % during 25 days. More sustained decrease in IOP  
269 was shown by sample PCL40 (16.9 %) and PCL10 (23.7 %) during the 30  
270 days of test. The decrease in IOP obtained with the disks was comparable  
271 with the one obtained by applying Trusopt eyedrops ( $p \geq 0.17$  for all disks).  
272 A decrease of at least 20% is desired in order to reduce the rate of open angle  
273 glaucoma-related damage [21].

274 Fig. 2(a) and Fig. 2(b) present IOP change in hypertensive eyes with  
275 implanted disks and in eyes treated with Trusopt<sup>®</sup> (Fig. 2(c)). PCL40  
276 presented a decrease of 41.1 % after 1 month and a decrease of 33.2 % after  
277 2 months, which is particularly suitable for patients with moderate to severe  
278 glaucoma [21]. IOP values in eyes with PCL40 implants are expected to  
279 approach the baseline values after approximately 3 months (see Fig. 1(b)).  
280 Samples PCL10 and 6%Lu,PCL40 showed similar IOP decrease percentages  
281 and peak IOP percentage in hypertensive eyes, while peak IOP was attained  
282 faster for sample 6%Lu,PCL40 due to faster drug release (see section 3.3).  
283 Thus, the release rate from the disks can be manipulated by blending in order  
284 to achieve the desired decrease in IOP.

285 Table 4 presents the average IOP decrease percentages achieved by the  
286 implanted disks in normotensive and hypertensive eyes, while Table 5 shows

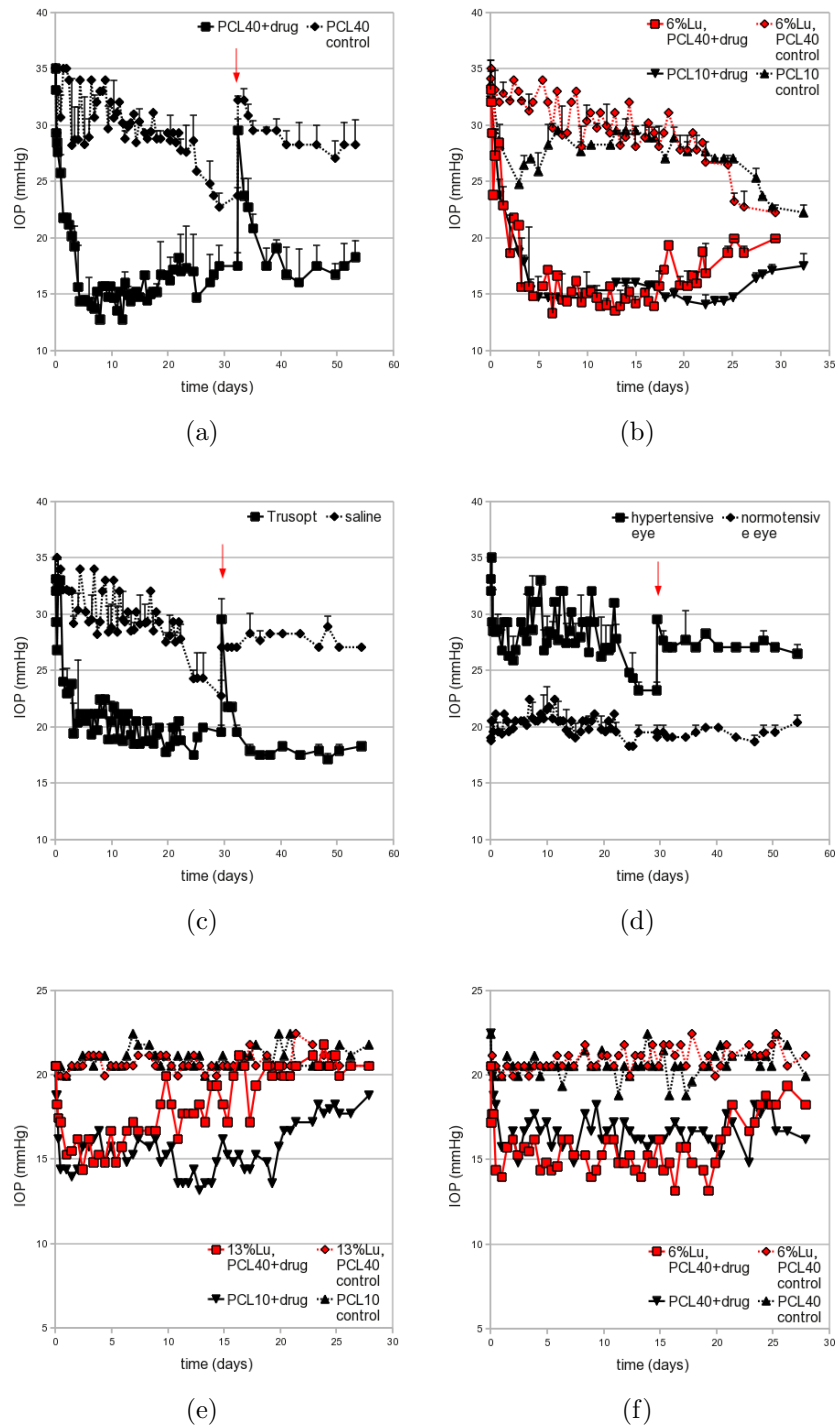


Figure 2: a), b) IOP in hypertensive eyes of group undergoing implant treatment, c) IOP in hypertensive eyes of group undergoing Trusopt<sup>®</sup> eyedrops treatment, d) IOP in glaucoma model group, e), f) IOP in normotensive eyes of group undergoing implant treatment (the red arrow indicates the point when a second cauterization was performed)

Sample	Peak IOP reduction (%) / time (days)		
	Normotensive eyes	Hypertensive eyes	
	1 month	1 month	2 months
Trusopt	27.85/0.96	36.59 (2.37)/3.38	35.33 (3.65)/34.56
PCL40	25.67/7.35	55.26 (0.98)/6.90	43.24 (2.55)/25.06
PCL10	35.92/6.90	50.21 (0.00)/6.94	-
6%Lu,PCL40	32.00/4.38	55.23 (5.03)/3.18	-
13%Lu,PCL40	29.96/2.42	-	-

Table 5: Peak IOP and the time interval from instillation/implantation to peak IOP

287 the peak IOP decrease and the time interval from instillation/implantation  
 288 to peak IOP. It can be noted that there was a higher IOP decrease in hy-  
 289 pertensive eyes than in normotensive eyes for eyedrops and disks ( $p \leq 0.01$   
 290 for all disks). Sample PCL40 showed the best performance in vivo (constant  
 291 decrease in IOP for longer time) due to more sustained drug release. The  
 292 obtained values for IOP decrease with Trusopt<sup>®</sup> are in agreement with litera-  
 293 ture values for normotensive ([22, 23]) and hypertensive eyes ([24, 25]). There  
 294 was a higher decrease in IOP for eyes treated with disks than in those treated  
 295 with eyedrops ( $p \leq 0.01$  for all disks) probably because of higher amounts of  
 296 drug released by the disks (average in vitro release rate of 0.43 (0.04) mg/day  
 297 for PCL40 or 1.34 (0.12) mg/day for PCL10 during 1 month versus 0.02  
 298 mg/day delivered by eyedrops ([19])). The changes in IOP obtained in the  
 299 eyes with implanted disk are similar to those obtained with the Ocusert drug  
 300 delivery system ([26]). Trusopt<sup>®</sup> eyedrops produced the fastest decrease in  
 301 IOP in normotensive eyes with peak IOP attained after 0.96 days, followed by  
 302 blend disks in agreement with in vitro release results (peak IOP was reached  
 303 fastest for blend disks with higher content of Lu). In hypertensive eyes, the  
 304 same trend in IOP decrease was maintained, but the average IOP and peak  
 305 IOP values were higher than those obtained in normotensive eyes. Peak IOP  
 306 occurred at similar times in hypertensive eyes, except for Trusopt<sup>®</sup>. Prob-  
 307 ably, dorzolamide administered by eyedrops might require multiple doses to  
 308 build up to steady state levels of concentration in the ciliary processes that  
 309 are required for IOP decrease in hypertensive eyes.

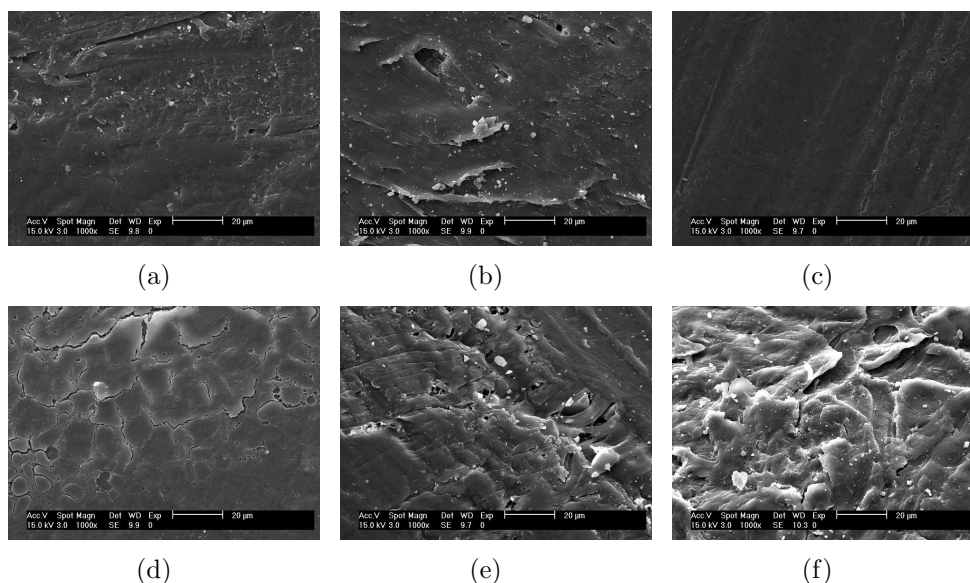


Figure 3: SEM of disks (with drug) surface. a) PCL40 as prepared, b) PCL40 in vivo, c) PCL10 as prepared, d) PCL10 in vivo, e) 6%Lu,PCL40 as prepared, f) 6%Lu,PCL40 in vivo

### 310 3.5. Morphology and drug distribution, SEM and EPMA

311 SEM and EMPA were performed in order to determine the morphology  
 312 of the disks and the drug distribution inside the disks before and after the in  
 313 vivo implantation.

314 Fig. 3(a) to Fig. 3(f) show the surface morphology of the prepared disks  
 315 and in vivo degraded disks. There are significant signs of degradation on the  
 316 implanted disk surface such as pores (Fig. 3(b)), cracks (Fig. 3(d)) and scales  
 317 (Fig. 3(f)). The in vitro degraded samples showed fewer signs of material  
 318 cracking (images not shown). This suggested enhanced degradation in vivo  
 319 in comparison with in vitro conditions (see section 3.7).

320 After preparation, the disks presented a heterogeneous drug distribution  
 321 (Fig. 4(a)) probably because of phase separation between drug and polymers  
 322 due to the high drug loading. After in vivo testing, there was almost no drug  
 323 at the surface (Fig. 4(b)), while in the disk cross-section there were still  
 324 significant amounts of drug present in sample PCL40 after 1 month in vivo  
 325 (Fig. 4(c)). The mapping of the other disks sections show that the release  
 326 was complete after 1 month of implantation.

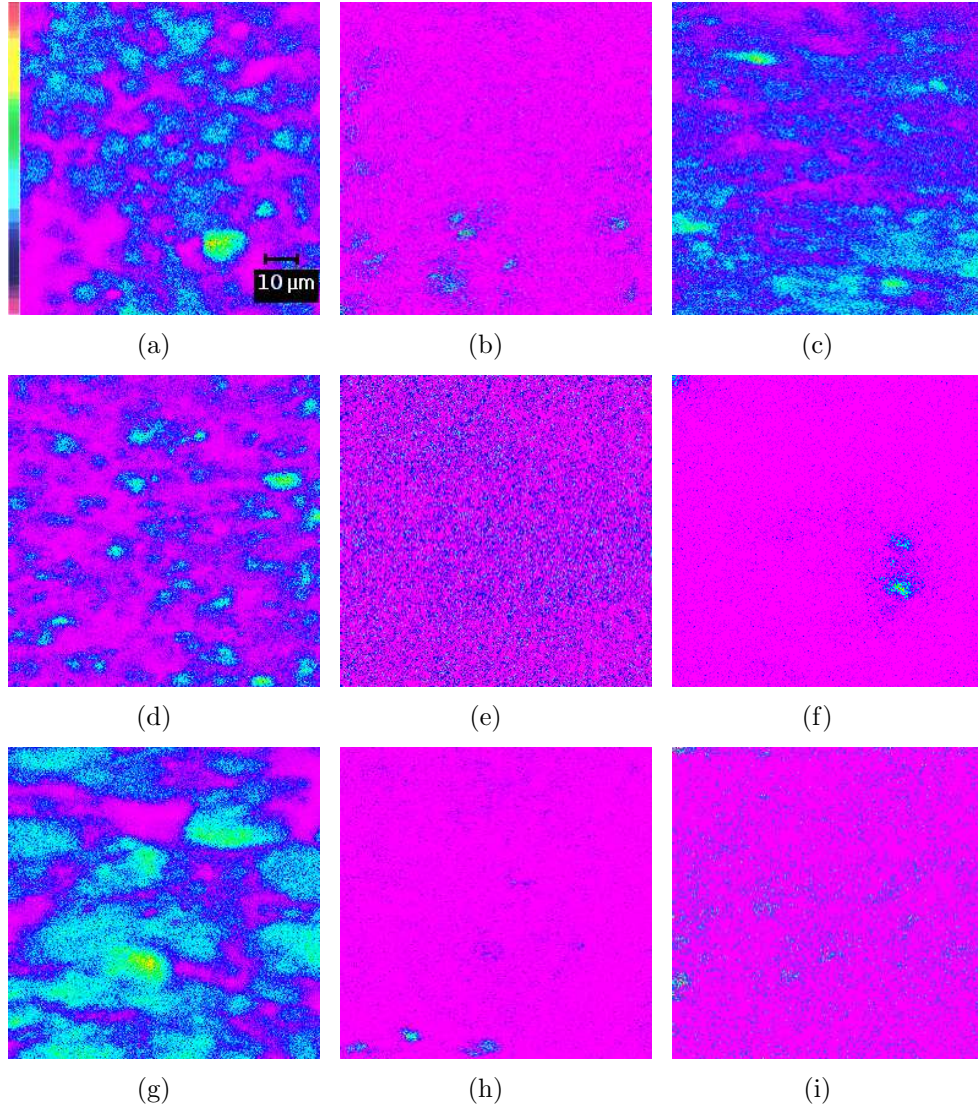


Figure 4: Sulphur drug mapping after 1 month in vivo. a) PCL40 surface as prepared, b) PCL40 surface in vivo, c) PCL40 section in vivo, d) PCL10 surface as prepared, e) PCL10 surface in vivo, f) PCL10 section in vivo, g) 6%Lu,PCL40 surface as prepared, h) 6%Lu,PCL40 surface in vivo, i) 6%Lu,PCL40 section in vivo (in the scale bar, the colour gradient represents 0% drug (pink) and 100% drug (red))



327 *3.6. In vitro and in vivo degradation*

328 To differentiate between a physical or a chemical degradation mecha-  
329 nism, the crystallinity and MW was determined for initial, in vitro and in  
330 vivo degraded samples (in section 6, the table 6 presents the change of disk  
331 crystallinity and MW due to in vitro and in vivo degradation). There was  
332 MW decrease due to chemical hydrolysis for PCL40+drug sample both after  
333 1 month and 2 months and for 6%Lu,PCL40+drug after 1 month. Sample  
334 PCL10+drug did not degrade in vivo probably due to higher initial crys-  
335 tallinity as crystalline regions are more inaccessible to water uptake. The  
336 MW of the in vitro degraded samples was also determined, but the obtained  
337 differences were not statistically significant ( $p \geq 0.17$ ). The samples presented  
338 lower crystallinity than the pure polymers (50.26 (0.33) % for PCL40 and  
339 68.51 (2.12) % for Lu) and the drug loaded samples showed lower crystallinity  
340 than the control samples probably due to co-crystallization of dorzolamide  
341 (that is above the solubility limit in the polymer). In general, there was an  
342 increase in crystallinity for in vitro and in vivo degraded samples because the  
343 amorphous regions are degraded first and because during drug elution, the  
344 mobile polymer chains rearrange themselves and crystallize [15, 20]. Crys-  
345 tallinity was higher only for some in vivo degraded samples with respect to  
346 the in vitro degraded samples, suggesting that there is crystallinity increase  
347 and enhanced mechanical breakdown in vivo (see section 3.7).

348 *3.7. Histologic evaluation*

349 The tissue samples collected from various organs showed normal cell mor-  
350 phology. The histological analysis of the tissues from the implantation site  
351 showed rapid resolution of the acute and chronic inflammatory stages and  
352 the development of normal foreign body reaction, consisting of adherent  
353 macrophages (Fig. 5(b)), fibroblasts, lymphocytes and foreign body giant  
354 cells (Fig. 5(c)) on the surface of the disk and fibrous capsule formation  
355 (Fig. 5(d)). Blood vessels (Fig. 5(a)) that formed in the fibrous capsule  
356 were also observed. There was a higher density of cells on the drug loaded  
357 disk with respect to control disks. No acute and/or chronic inflammation  
358 was seen after 2 months, indicating that the disks were biocompatible and  
359 did not produce inflammatory reactions characteristic to toxic materials.

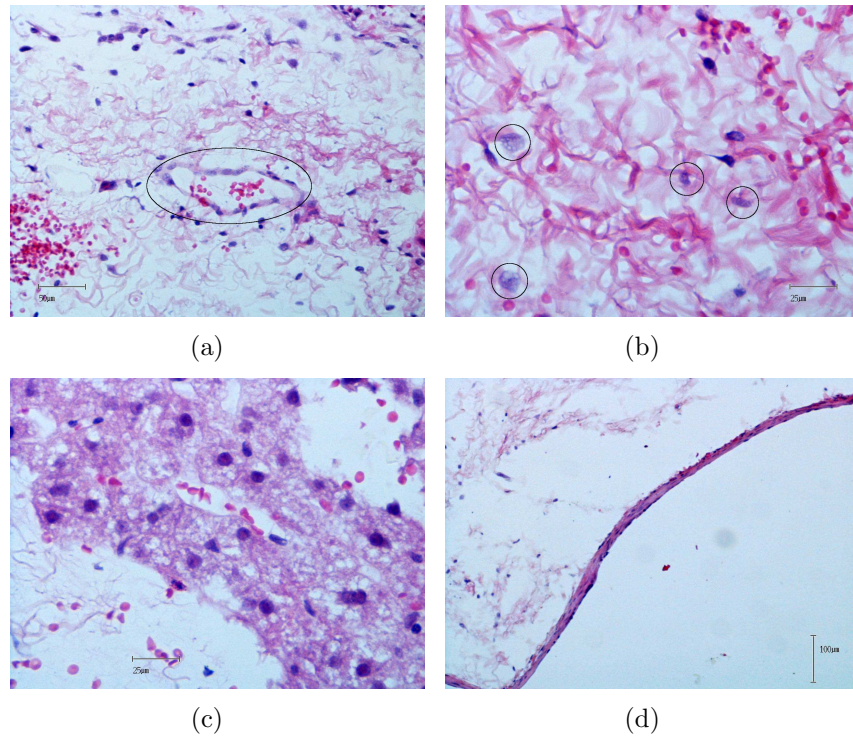


Figure 5: Light microscopy images of implanted disk showing a) cells and blood vessel (shown in the ellipse); b) macrophage cells (highlighted by circles); c) foreign-body giant cell; d) fibrous capsule

#### 360 4. Conclusions

361 Subconjunctival disks based on PCL and loaded with dorzolamide hydrochloride were implanted in rabbit eyes and their in vivo performance was  
 362 assessed by their capacity to lower IOP in normotensive and hypertensive  
 363 eyes. The high MW PCL showed non-cumulative release rates above the  
 364 therapeutic level during 3 months. Histologic analysis showed normal foreign  
 365 body reaction response consisting of adherent macrophages, fibroblasts,  
 366 lymphocytes, foreign body giant cells and fibrous capsule formation. The  
 367 release kinetics suggested a three stage release mechanism based on drug  
 368 diffusion, polymer erosion and polymer degradation, with different steps  
 369 depending on disk composition. In vivo, the fibrous capsule formation around  
 370 the PCL implant controls the drug release, working as a barrier membrane.  
 371 For blend disks, due to polymer erosion that takes place mostly in the first  
 372

373 day of release, the fibrous capsule/barrier control is absent.

374 In normotensive eyes, a 20 % decrease in IOP obtained with the disks  
375 during 1 month was comparable with the one obtained by applying Trusopt<sup>®</sup>  
376 eyedrops. In hypertensive eyes, higher decrease percentages (around 40 %)   
377 were obtained for all samples, with the most sustained decrease from the  
378 high MW PCL (40 % after 1 month, 30 % after 2 months). Peak IOP  
379 occurred earlier for blend disks due to enhanced drug release triggered by  
380 polymer erosion. It was proven that the devices can lower IOP in sustained  
381 manner in a rabbit glaucoma model. The blending offers the possibility to  
382 manipulate release rate and the amount of released drug in order to prepare  
383 devices tailored to the needs of patients (target IOP decrease percentages  
384 should take into account risk factors and disease progression).

## 385 5. Acknowledgements

386 The authors would like to thank Merck Sharp & Dohme Portugal for  
387 kindly supplying dorzolamide hydrochloride and Trusopt<sup>®</sup> eyedrops. FCT  
388 (Fundação para a Ciência e a Tecnologia) financial support is acknowledged  
389 by Mădălina V. Natu (SFRH/BD/30198/2006).

## 390 References

- 391 [1] H A Quigley (2005) Glaucoma: Macrocosm to Microcosm. Invest. Oph-  
392 thalmol. Vis. Sci., doi:10.1167/iovs.041070
- 393 [2] K. Schwartz, D. Budenz (2004) Current management of glaucoma, Curr.  
394 Opin. Ophthalmol., 15, 119-126
- 395 [3] P.T. Khaw, P. Shah, A.R. Elkington (2004) Glaucoma-2: Treatment,  
396 Br. Med. J., doi:10.1136/bmj.328.7432.156
- 397 [4] E.M. del Amo, A. Urtti (2008) Current and future ophthalmic drug  
398 delivery systems A shift to the posterior segment, Drug Discov. Today,  
399 doi:10.1016/j.drudis.2007.11.002
- 400 [5] J.M. Korte, T. Kaila, K.M. Saari (2002) Systemic bioavailability and  
401 cardiopulmonary effects of 0.5% timolol eyedrops. Graefes Arch. Clin.  
402 Exp. Ophthalmol., doi:10.1007/s00417-002-0462-2

- 403 [6] R.J. Noecker (2005) Evaluation of Bimatoprost 0.03% versus La-  
404 tanoprost 0.005%: A Paired Comparison Study. *Invest. Ophthalmol.*  
405 *Vis. Sci.*, 46, E-Abstract 2452.
- 406 [7] S.V. Kulkarni, K.F. Damji, Y.M. Buys (2008) Medical management  
407 of primary open-angle glaucoma: Best practices associated with en-  
408 hanced patient compliance and persistency. *Patient Prefer. Adherence*,  
409 2, 303313
- 410 [8] B.K. Nanjawade, F.V. Manvi, A.S. Manjappa (2007) In situ-forming  
411 hydrogels for sustained ophthalmic drug delivery, *J. Con. Rel.*,  
412 doi:10.1016/j.jconrel.2007.07.009
- 413 [9] J.L. Bourges, C. Bloquel, A. Thomas, F. Froussart, A. Bochot, F. Azan,  
414 R. Gurny, D. BenEzra, F. Behar-Cohen (2006) Intraocular implants for  
415 extended drug delivery: Therapeutic applications. *Adv. Drug. Deliv.*  
416 *Rev.*, doi:10.1016/j.addr.2006.07.026
- 417 [10] M.V. Natu and M.N. Gaspar and C.A.F. Ribeiro and I.J. Correia and  
418 D. Silva and H.C. de Sousa and M.H. Gil (2011) A poly( $\epsilon$ -caprolactone)  
419 device for sustained release of an anti-glaucoma drug, *Biomed. Mater.*,  
420 6, 025003, doi: 10.1088/1748-6041/6/2/025003
- 421 [11] T. Yasukawa and Y. Ogura and E. Sakurai and Y. Tabata and  
422 H. Kimura (2005) Intraocular sustained drug delivery using im-  
423 plantable polymeric devices, *Adv. Drug Deliv. Rev.*, 57, 2033–2046, doi:  
424 10.1016/j.addr.2005.09.005
- 425 [12] N. Kuno and S. Fujii (2010) Biodegradable intraocular therapies  
426 for retinal disorders: progress to date, *Drugs Aging*, 27, 117–134,  
427 DOI:10.2165/11530970-000000000-00000
- 428 [13] J. Breitenbach (2002) Melt extrusion: from process to drug delivery  
429 technology, *Eur. J. Pharm. Biopharm.*, 54, 107–117
- 430 [14] M.V. Natu, M.H. Gil, H.C. de Sousa (2008) Supercritical solvent im-  
431 pregnation of poly( $\epsilon$ -caprolactone)/poly(oxyethylene-b-oxypropylene-  
432 b-oxyethylene) and poly( $\epsilon$ -caprolactone)/poly(ethylene-vinyl ac-  
433 etate) blends for controlled release applications. *J. Sup. Fluids*,  
434 doi:10.1016/j.supflu.2008.05.006

- 435 [15] M.V. Natu, H.C. de Sousa, M.H. Gil (2010) Effects of drug solubil-  
436 ity, state and loading on controlled release in bicomponent electrospun  
437 fibers. *Int. J. Pharm.*, doi:10.1016/j.ijpharm.2010.06.045
- 438 [16] C.G. Pitt, F.I. Chasalow, Y.M. Hibionada, D.M. Klimas, A. Schindler  
439 (1981) Aliphatic polyesters. I. The degradation of poly( $\epsilon$ -caprolactone)  
440 in vivo, *J. Appl. Polym. Sci.*, doi:10.1002/app.1981.070261124
- 441 [17] H. Levkovitch-Verbin, H.A. Quigley, K.R.G. Martin, D. Valenta, L.A.  
442 Baumrind, M.E. Pease (2002) Translimbal Laser Photocoagulation to  
443 the Trabecular Meshwork as a Model of Glaucoma in Rats, *Invest. Oph-*  
444 *thalmol. Vis. Sci.*, 43, 402-410.
- 445 [18] J. Ruiz-Ederra, A.S. Verkman (2006) Mouse model of sustained elevation  
446 in intraocular pressure produced by episcleral vein occlusion. *Exp. Eye*  
447 *Res.*, doi:10.1016/j.exer.2005.10.019
- 448 [19] K. Schmitz, P. Banditt, M. Motschmann, F. P. Meyer, W. Behrens-  
449 Baumann (1999) Population Pharmacokinetics of 2% Topical Dorzo-  
450 lamide in the Aqueous Humor of Humans, *Invest. Ophthalmol. Vis. Sci.*,  
451 40, 1621-1624.
- 452 [20] M. Miyajima, A. Koshika, J. Okada, M. Ikeda, K. Nishimura (1997)  
453 Effect of polymer crystallinity on papaverine release from poly(L-lactic  
454 acid) matrix. *J. Con. Rel.*, doi:10.1016/S0168-3659(97)00081-3
- 455 [21] L. Yudcovitch, Pharmaceutical, Laser and Surgical Treatments for  
456 Glaucoma: An Update, [http://www.pacificu.edu/optometry/ce/  
457 courses/15166/pharglapg2.cfm#Pharmaceutical](http://www.pacificu.edu/optometry/ce/courses/15166/pharglapg2.cfm#Pharmaceutical), Accessed October  
458 15, 2010.
- 459 [22] A. Harris, O. Arend, H.S. Chung, L. Kagemann, L. Cantor, B. Martin  
460 (2000) A comparative study of betaxolol and dorzolamide effect on oc-  
461 ular circulation in normal-tension glaucoma patients. *Ophthalmol.*, 107,  
462 430-434
- 463 [23] A. Scozzafava, L. Menabuoni, F. Mincione, F. Briganti, G. Min-  
464 cione, C.T. Supuran (1999) Carbonic Anhydrase Inhibitors. Synthesis of

- 465 Water-Soluble, Topically Effective, Intraocular Pressure-Lowering Aro-  
466 matic/Heterocyclic Sulfonamides Containing Cationic or Anionic Moi-  
467 eties: Is the Tail More Important than the Ring? *J. Med. Chem.*,  
468 doi:10.1021/jm9900523
- 469 [24] A.G. Konstas, V.P. Kozobolis, S. Tsironi, I. Makridaki, R. Efre-  
470 mova, W.C. Stewart (2008) Comparison of the 24-hour intraocu-  
471 lar pressure-lowering effects of latanoprost and dorzolamide/timolol  
472 fixed combination after 2 and 6 months of treatment. *Ophthalmol.*,  
473 doi:10.1016/j.opthta.2007.03.007
- 474 [25] M. Seki, T. Tanaka, H. Matsuda, T. Togano, K. Hashimoto, J.  
475 Ueda, T. Fukuchi, H. Abe (2005) Topically administered timolol and  
476 dorzolamide reduce intraocular pressure and protect retinal ganglion  
477 cells in a rat experimental glaucoma model. *Br. J. Ophthalmol.*,  
478 doi:10.1136/bjo.2004.052860
- 479 [26] K.L. Macoul, D. Pavan-Langston (1975) Pilocarpine Ocusert System  
480 for Sustained Control of Ocular Hypertension. *Arch. Ophthalmol.*, 93,  
481 587-590

## 482 6. Supplementary information

Sample	As prepared	In vitro		In vivo					
	$X_{rel}$ (%)	$X_{rel}$ (%)	mass loss (%)	$X_{rel}$ (%)	mass loss (%)	$M_w$ (g/mole)		$\Delta M_w$ (%)	
		1 month		1 month		1 month	2 months	1 month	2 months
PCL40+drug	36.97 (1.93)	29.13 (0.97)	13.46 (1.14)	38.89 (0.03)†	15.07 (4.93)	62377.5 (725.5)	60274.5 (112.4)	4.9*	8.1*
PCL40	50.26 (0.33)	43.62 (1.27)	0.74 (0.11)	46.13 (1.62)	0.90 (0.07)	62727.3 (3555.6)	57653.5 (210.0)	4.4	12.1*
PCL10+drug	40.06 (0.15)	42.26 (4.36)	22.68 (1.76)	50.66 (1.48)	30.75 (1.19)	16906.5 (2556.2)	-	10.8	
PCL10	56.41 (0.34)	-	1.73 (0.42)	60.85 (1.51)	2.98 (0.21)	15152.5 (55.9)	-	0.7	-
6%Lu,PCL40+drug	32.12 (0.17)	38.51 (0.72)	36.77 (0.01)	47.18 (0.70)†	33.37 (0.48)	60625.5 (102.5)	-	7.6*	-
6%Lu,PCL40	43.41 (0.19)	-	1.30 (0.10)	45.15 (1.79)	1.51 (0.14)	58144.5 (748.8)	-	11.4*	-
13%Lu,PCL40+drug	30.32 (0.52)	41.43 (0.56)	41.12 (0.45)	44.07 (2.69)	37.36	61636.5 (2686.3)	-	6.0	-
13%Lu,PCL40	38.40 (1.13)	-	7.71 (0.56)	44.43 (2.96)	5.84	61606	-	6.1	-

Table 6: Crystallinity, mass loss and molecular weight evolution for in vitro and in vivo degraded samples ( $p \leq 0.05$ , \*, relative to initial MW, †, relative to in vitro crystallinity)